Positional importance of Pro^{53} adjacent to the Arg^{49}-Gly^{50}-Asp^{51} sequence of rhodostomin in binding to integrin αIIbβ3

Chih-Pei CHANG*, Jui-Chin CHANG*, Hsin-Hou CHANG*[1], Wei-Jern TSAI† and Szecheng J. LO*[2]

*Institute of Microbiology and Immunology, National Yang-Ming University, 155 Li-nan Street, Sec. 2, Shih-Pai, Taipei 11221, Taiwan, and †National Research Institute of Chinese Medicine, 155-1 Li-nan Street, Sec. 2, Shih-Pai, Taipei 11221, Taiwan

Rhodostomin (RHO), a disintegrin isolated from snake venom, has been demonstrated to inhibit platelet aggregation through interaction with integrin αIIbβ3, but there is a lack of direct evidence for RHO–integrin αIIbβ3 binding. In addition, no study on the length of Arg^{49}-Gly^{50}-Asp^{51} (RGD) loop of RHO influencing on its binding to integrin αIIbβ3 has been reported. In the present study we have developed a highly sensitive dot-blot and glutathione S-transferase–RHO pull-down assays; the latter was coupled with a biotin–avidin–horseradish peroxidase enhanced-chemiluminescence detection system. These were able to demonstrate the direct binding of RHO to integrin αIIbβ3. The pull-down assay further showed that four alanine-insertion mutants upstream of the RGD motif and three insertions downstream of the RGD were able to decrease integrin αIIbβ3 binding activity to only a limited extent. By contrast, two insertions immediately next to RGD and one insertion in front of the Cys^{57} caused almost complete loss of binding activity to αIIbβ3. The results of the platelet-aggregation-inhibition assay and platelet-adhesion assay for the insertion mutants were consistent with results of the pull-down assay. It is thus concluded that, although an insertion of a single alanine residue in many positions of the RGD loop has only minor effects on RHO binding to integrin αIIbβ3, the specific position of Pro^{53} residue adjacent to the RGD sequence is important for RHO binding to platelet integrin αIIbβ3.

Key words: disintegrin, insertion mutagenesis, pull-down assay.

INTRODUCTION

The integrins, a superfamily of structurally related $\alpha\beta$ heterodimers, represent a major class of adhesion receptors. In vertebrates, especially in mammals, integrin-mediated signals regulate cell–cell and cell–extracellular matrix interactions which are important in embryonic development, morphogenesis, differentiation, homoeostasis, wound healing, immune-system function and tumour metastasis (for reviews, see [1–7]). To date, 15 α subunits and eight β subunits have been found, and more than 22 integrin heterodimers have been identified. Integrin αIIbβ3 is the most abundant adhesive receptor on the platelet surface, each platelet having about 80000 integrin αIIbβ3 molecules [8].

Intense studies have been made to define the integrin recognition sites in the ligands of αIIbβ3. The first defined binding motif of αIIbβ3 was the Arg-Gly-Asp (RGD in the one-letter amino acid notation) sequence, which is present in fibronectin, fibrinogen, von Willebrand factor (vWF), vitronectin and a variety of adhesive proteins [2,9]. However, the RGD motif is also recognized by other species of integrins as well, i.e., αvβ1 and αvβ3 [10]. From the studies of synthetic fibronectin fragments and by substitution at the flanking sequence of RGD, it has been revealed that the surrounding sequence of the RGD motif is also important in integrin binding specificity and affinity [11–13]. However, the effects of relative distance between RGD motif and flanking sequence or residues have not been determined.

Disintegrins are soluble non-enzymic small proteins from snake venom that inhibit platelet aggregation via the occupancy of fibrinogen-binding receptors (integrin αIIbβ3) (for reviews, see [14–17]). Up to the present, more than 25 snake-venom disintegrins have been isolated. The structural features of snake disintegrins are that they are low-molecular-mass, cysteine-rich and RGD-containing peptides. Rhodostomin (also known as kistrin) is found in the venom of *Agkistrodon* (*Calloselasma*) *rhodostoma* (Malayan pit viper) and contains 68 amino acid residues with 12 cysteine residues and an RGD sequence at the positions 49–51 [18]. It has been shown to be one of the strongest antagonists to platelet aggregation among the disintegrin family [18–20]. The K_d of rhodostomin binding to purified αIIbβ3 is about 100 nM, to the resting platelets is 10.8 nM and to the ADP-activated platelets is 1.7 nM [19]. A study by alanine scanning mutagenesis has proved that the RGD motif of rhodostomin is the major region responsible for integrin αIIbβ3 binding [21]. Studies of rhodostomin and other disintegrins have also suggested that the amino acids flanking RGD provide a protrusive structure that influences integrin binding affinity and specificity [22–25]. Nevertheless, no direct binding of integrin αIIbβ3 by rhodostomin (RHO) has been shown.

In the present study we have established a system of glutathione S-transferase (GST) pull-down assay of biotin-labelled integrin and coupled this to a highly sensitive detection method using avidin–horseradish peroxidase (HRP)-enhanced chemiluminescence (ECL®; Amersham) to analyse RHO binding to integrins.

Abbreviations used: RHO, rhodostomin; GST, glutathione S-transferase; HRP, horseradish peroxidase; ECL® (Amersham), enhanced chemiluminescence; RGD, the motif Arg-Gly-Asp in one-letter amino acid notation; vWF, von Willebrand factor; PKA, protein kinase A; NIH, National Institutes of Health.

[1] Present address: Graduate Institute of Molecular and Cellular Biology, Tzu-Chi University, Hualien, Taiwan.
[2] To whom correspondence should be addressed (e-mail losj@ym.edu.tw).

This assay system was successfully employed to elucidate the effect of amino acid position and of specific residues on RHO when binding to integrin αIIbβ3.

MATERIALS AND METHODS

Materials

Reagents were purchased from Sigma (St Louis, MO, U.S.A.) unless indicated. Sulfo-NHS-Biotin was purchased from Pierce (Rockford, IL, U.S.A.). GSH–Sepharose 4B and the ECL® detection kit were from Amersham Pharmacia Biotech (Uppsala, Sweden). Antibodies were purchased from Chemicon (Temecula, CA, U.S.A.).

Plasmids for the expression of RHO and its mutants

The plasmids expressing GST–RHO, namely pGST-RHO(RGD), pGST-RHO(RGE), pGSTag-RHO(RGD), and pGSTag-RHO(RGE), were as described previously [26,27]. The alanine insertion GST–RHO mutants were generated by replacement into pGST-RHO(RGD) by PCR amplification. The designation of mutants correspond to the position of the inserted alanine residue. For example, GST–RHO(45+A) and GST–RHO(46+A) are alanine insertions after the position 45 and 46 respectively. For simplicity, they are abbreviated to '45+A' and '46+A'.

Preparation of the GST-fusion proteins

Production of the GST-fusion proteins was by 0.1 M isopropyl 1-thio-β-D-galactopyranoside induction in *Escherichia coli* JM109 [28]. Proteins were purified from the bacterial lysate by using GSH–Sepharose 4B beads. After washing, the bound GST-fusion proteins were eluted with elution buffer (10 mM GSH in 50 mM Tris/HCl, pH 8.0). The concentration of purified GST-fusion proteins was determined by the Bio-Rad Protein Assay kit (Bio-Rad, Richmond, CA., U.S.A.) and adjusted to 10 μM with elution buffer.

Preparation of platelets

Platelets were isolated by using the methods described previously [29]. In brief, human blood was collected from six healthy individuals (three males and three females, 25–32 years old) who had not taken medication for at least 2 weeks and had been well rested before being bled. The blood was drawn into acid-citrate/dextrose and was centrifuged at 150 ***g*** for 30 min to obtain platelet-rich plasma. Platelet-rich plasma was centrifuged at 1000 ***g*** for 1 min to remove the remaining red blood cells. The platelet-rich plasma was re-centrifuged at 1000 ***g*** for 15 min. The platelet pellet was resuspended in a volume of Ca^{2+}-free Tyrode's buffer with apyrase (1 unit/ml) equal to the starting volume of the blood and incubated at 37 °C for 30 min. The platelet suspension was centrifuged at 1000 ***g*** for 15 min, discarding the supernatant fluid, and then the platelets were gently resuspended in a suitable volume of Ca^{2+}-containing Tyrode's buffer.

GST pull-down assay

Intact platelets were first labelled by Sulfo-NHS-Biotin. The biotinylated platelets were then disrupted by 0.5% Triton X-100 in 50 mM Tris/HCl/150 mM NaCl/1 mM $MgCl_2$/1 mM $CaCl_2$/1 mM $MnCl_2$, pH 7.4. The platelet lysate was centrifuged at 8000 ***g*** for 15 min to remove unbroken platelets. The suspension was pre-cleared with GSH–Sepharose 4B. The pre-cleared platelet lysate was then pulled down by GST-fusion-protein-coated GSH–Sepharose 4B beads. The pull-down proteins were analysed by SDS/9% PAGE. After electrophoresis, the proteins were transferred to a PVDF membrane and detected with avidin–HRP and ECL®.

Western blotting

Western blotting was performed as previously described [30]. In brief, the pull-down proteins were analysed by SDS/9%-PAGE and transferred to a PVDF membrane. The pull-down proteins were detected by rabbit anti-(human β_3) polyclonal antibody (AB1932, Chemicon) and peroxidase-conjugated anti-(rabbit IgG) antibody or mouse anti-(human αIIb) monoclonal antibody (MAB1990; Chemicon) and peroxidase-conjugated anti-(mouse IgG) antibody.

Platelet-aggregation-inhibition assay

Human platelets prepared as previously described were adjusted to 5×10^7 cells/ml. Platelet aggregation was measured with a four-chambered platelet aggregation chromogenic kinetic system (PACKS-4; Helena Laboratories, Beaumont, TX, U.S.A.). Platelets were incubated with the indicated concentrations of GST-fusion proteins at 37 °C for 2 min, then induced with thrombin [final concn. 0.4 National Institutes of Health (NIH) units/ml] to aggregate. The GST-fusion proteins were diluted with PBS to a suitable concentration for experiments.

Platelet-attachment assay

The platelet-attachment assay was performed according to the previously established method with a slight modification [31]. In brief, 1.0 μM GST-fusion proteins were coated on coverslips at 37 °C for 2 h. After washing, the uncoated region of coverslips were blocked with 5% BSA in PBS, pH 7.4, at 4 °C for 6 h. Cells were adjusted to 1×10^6 cells/ml and incubated with the GST-fusion-protein-coated coverslips at 37 °C for 15 min. The coverslips were then gently washed three times with PBS to remove unattached cells. The attached cells were fixed by 0.5% glutaraldehyde and stained with Liu's stain [32].

RESULTS AND DISCUSSION

RHO binds to both intact and detergent-solubilized platelets

We demonstrated previously that the GST-fusion RHO, GST–RHO(RGD), is bioactive for inducing platelet adhesion and facilitating cell-line adhesion [27,31]. In order to obtain direct biochemical evidence of RHO–integrin αIIbβ3 binding, we expressed two GST–RHO derivatives, GSTag-RHO(RGD) and GSTag-RHO(RGE), which can be labelled by protein kinase A (PKA) in the presence of [γ-^{32}P]ATP *in vitro* [27]. The ^{32}P-labelled proteins were then used as probes to detect their binding to intact cells or Triton X-100-solubilized membrane fractions, which were dotted on to nitrocellulose papers. The results shown in Figure 1 indicate clearly that both intact and detergent-solubilized platelets can be bound by GSTag-RHO(RGD), but not the other cells, such as HeLa, HuH-7, HepG2, NIH3T3, B16 and red blood cells. The amount of GSTag-RHO(RGD) bound, reflected by the intensity of autoradiograph, is proportional to the amount of loaded platelets (Figure 1A, line 1) and platelet lysate (Figure 1B). There is no binding signal from GSTag-RHO(RGE), and these results suggest that RHO binding to platelets is through an RGD–integrin interaction. Furthermore,

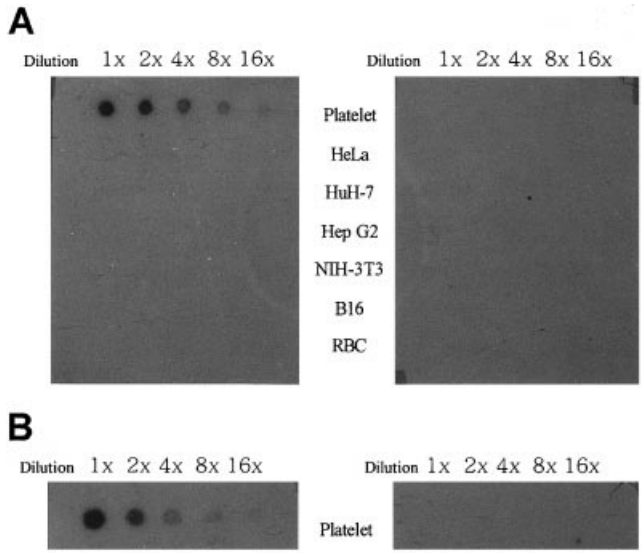

Figure 1 Dot-blot analysis of RHO binding to intact and solubilized platelets

The left panels show the detection of [^{32}P]GSTag-RHO(RGD) binding to intact cells (**A**) and Triton X-100-soluablilized fraction (**B**). The right panels show the detection of [^{32}P]-GSTag-RHO(RGE) binding to intact cells (**A**) and Triton X-100-solubilized fraction (**B**). The dilutions are indicated at the top of blots. The applied cell number in the lane '1x' for platelet and red blood cells was 2.5×10^7 cells; for other cells it was 5×10^5 cells. Types of cells used in the assay are also indicated.

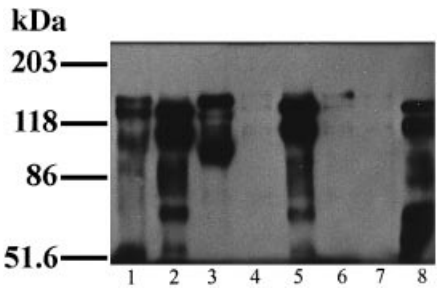

Figure 2 GST pull-down assays of biotinylated human platelet cell lysate

Biotinylated human platelet surface proteins were probed by avidin–HRP ECL®. Lane 1, total cell lysate of surface-biotinylated human platelets. Biotinylated platelet surface proteins were absorbed by GST–RHO(RGD) and analysed under reducing conditions (lane 2) and under non-reducing condition (lane 3) or absorbed by GST–RHO(RGE) (lane 4), by GST–RHO(RGD) in the presence of EDTA (lane 6) or kistrin (lane 7). The GST–RHO(RGE)-column cell-lysate flowthrough was reabsorbed by GST–RHO(RGD) (lane 5). The anti-(integrin β_3) antibody immunoprecipitated the biotinylated surface proteins, which were eluted from the GST–RHO(RGD) column (lane 8).

the platelet integrins in Triton X-100-solubilized lysate must remain functional to be bound by GST–RHO. It is possible, however, that the amount of integrins present in the five negative cell lines may be too low to be detected by ^{32}P-labelled RHO, although their adhesion could be mediated by GST–RHO interacting with integrin [27].

Direct interaction of solubilized platelet integrin αIIbβ3 and RHO

To obtain evidence of direct binding between RHO and integrin, the GST–RHO(RGD) or GST–RHO(RGE) were coated on to

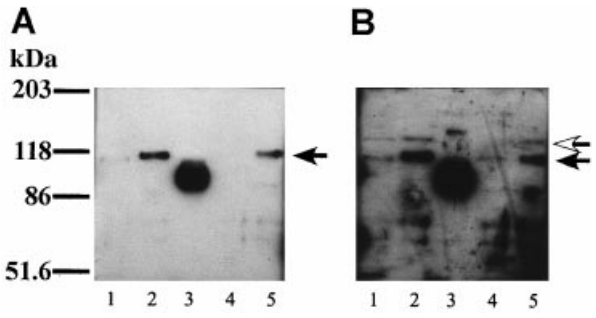

Figure 3 Western blotting analysis of GST–RHO pull-down assay

Biotinylated surface proteins on human platelets were absorbed by the GST–RHO column and detected by anti-(integrin β_3) antibody (**A**) and anti-(integrin β_3) antibody and anti-(integrin αIIb) antibody (**B**). Lane 1, platelet total lysate; lane 2, GST–RHO(RGD) pull-down (reducing conditions); lane 3, GST–RHO(RGD) pull-down (non-reducing conditions); lane 4, GST–RHO(RGE); the GST-RHO(RGE)-column cell-lysate flowthrough was reabsorbed by GST–RHO(RGD) (lane 5). The black arrowhead shows the integrin β3 subunit and the white arrowhead shows the integrin αIIb subunit.

GSH–Sepharose 4B beads and incubated with biotinylated platelet lysate (see the Materials and methods section). The bound proteins were analysed by SDS/PAGE and detected by avidin–HRP coupling with ECL®. Figure 2 shows that two major protein bands (110 and 130 kDa in size) and four other minor bands (in a size ranging from 50 to 80 kDa) were pulled down by GST–RHO(RGD), but not by GST–RHO(RGE) (lane 2 versus lane 4). The pull-down results are consistent with the previous studies [27,28,31] and support the result of dot-blot binding assay shown in Figure 1, strongly suggesting that the pull-down complex formed by GST–RHO(RGD) is specific.

When the GST–RHO(RGD) pull-down complex was analysed under non-reducing conditions, the four minor bands disappeared, while two major proteins shifted to the position of 95 kDa and 140 kDa (lane 3 vs. lane 2). The position shift under non-reducing conditions is a property of αIIbβ3 described in previous reports [2,33], giving a strong indication that the 95 kDa protein is β3 and the 140 kDa protein is αIIb. This supposition was supported by anti-β3 immunoprecipitation, which showed the same profile as the GST–RHO(RGD) pull-down (lane 8 versus lane 2). Confirmation that the 95 kDa protein is β3 and the 140 kDa protein is αIIb was obtained from Western blotting using anti-β3 and anti-αIIb antibodies (Figure 3). Since no protein was detected using GST–RHO(RGE), we would expect the integrin in the flow-through fraction of GST–RHO(RGE). This should be recoverable by GST–RHO(RGD)-coated beads. Results showed that those proteins were indeed recovered and gave the same profile as the direct pull-down assay by GST–RHO(RGD) (lane 5 versus lane 2). This further supports the suggestion that the pull-down complex is specific.

It is well known that ligand binding to αIIbβ3 is cation-dependent. We therefore added EDTA to the pull-down assay. No protein was observed when the assay was analysed by SDS/PAGE and ECL® (lane 6), indicating that GST–RHO(RGD) binding to complex is bivalent-cation-dependent and the complex contains integrins. Since the GST–RHO(RGD) binding complex can be competed out by native snake-venom kistrin (lane 7), this indicates that pull-down complex is via RHO binding rather than GST. Taking all the results shown in Figure 2 together, we have clearly demonstrated that RHO can directly and specifically bind to integrin αIIbβ3 *in vitro*.

RHO mutants created by alanine insertion at the N-terminal flanking sequence of RGD motif reduce integrin αIIbβ3 binding to a limited extent

To examine whether the length, the relative distance and any of the specific residues of flanking sequence around RGD in RHO play a role in the binding of αIIbβ3, we generated ten alanine-insertion mutants at both the N-terminal and C-terminal flanking sequence of the RGD motif (see Figures 4A and 5A). By using the GST pull-down assay, the αIIbβ3 binding activity of N-terminal insertion mutants, 45+A, 46+A, 47+A and 48+A, was determined (Figure 4D). When similar amounts of GST-fusion proteins were used (Figures 4B and 4C), all the four N-terminal insertion mutants can pull down αIIb and β3 (Figure 4D, lanes 4–7). The proportion of integrin αIIb and β3 pulled down by the N-terminal insertion mutants ranged from 30 to 56 % and from 8 to 54 % respectively of those pulled down by the wild-type GST–RHO(RGD) (lane 2, estimated by a densitometer). To confirm that the insertion-mutant-reduced binding to integrin αIIbβ3 was not due to an improper loading, the flow-through proteins from insertion and RGE mutants were then pulled down by GST–RHO(RGD)-coated beads and examined. The amount of αIIbβ3 recovered from insertion mutants was 4–6-fold higher than that from GST–RHO(RGD) flow-through (Figure 4E). The GST pull-down activity of these four insertion mutants is summarized in Table 1. Taking all the results together, we suggest that the placing of an extra alanine residue in front of RGD increases the length of loop and so reduces, but does not eliminate, binding to integrins.

RHO mutants created by alanine insertion downstream of the RGD motif lose αIIbβ3 binding activity

Integrin binding by six RHO mutants with alanine insertion at the C-terminus was also determined. Results of pull-down assay using a similar amount of GST-fusion proteins (Figures 5B and 5C) indicated that the mutants 51+A, 52+A and 56+A retained little or no protein (Figure 5D, lanes 4, 5 and 9). Three other mutants, 53+A, 54+A and 55+A, had reduced binding to αIIbβ3, compared with the wild-type RHO. The proportion of integrin αIIb pulled down was between 57 and 82 % of the wild-type and of integrin β3 pulled down was between 14 and 74 % of the wild-type (lanes 6, 7 and 8 versus lane 2, estimated by a densitometer). The result of secondary pull-down by GST–RHO(RGD) confirmed that the binding by mutants was not due to an improper loading (Figure 5E). The pull-down activity of these six insertion mutants relative to the wild-type is summarized in Table 1. These results suggested that the position of Pro^{53} relative to the RGD motif is extremely important for integrin binding because the two alanine-insertion mutants (51+A and 52+A) move Pro^{53} to position 54. This observation is supported by the fact that the pull-down result from a Met52 deletion mutant that has moved Pro^{53} to position 52 also completely lost αIIbβ3 binding activity (results not shown). In contrast, it would seem that the loss of function of 56+A is not due a shift of Cys^{57} to position 58, since the mutants 53+A, 54+A and 55+A, which all also cause a shift of Cys^{57} to position 58, still retained the binding capability.

Inhibition effect on thrombin-induced platelet aggregation was lost for mutants 51+A, 52+A and 56+A

Since the affinity state of integrin can be modulated by intracellular signal (inside-out signalling), in order to correlate the pull-down assay with biological function of various mutants we measured the inhibition effect of each mutants on thrombin-induced platelet aggregation. Results showed that only GST–RHO(RGD) inhibited thrombin-induced platelet aggregation in a dose-dependent manner. The seven insertion mutants, 45+A,

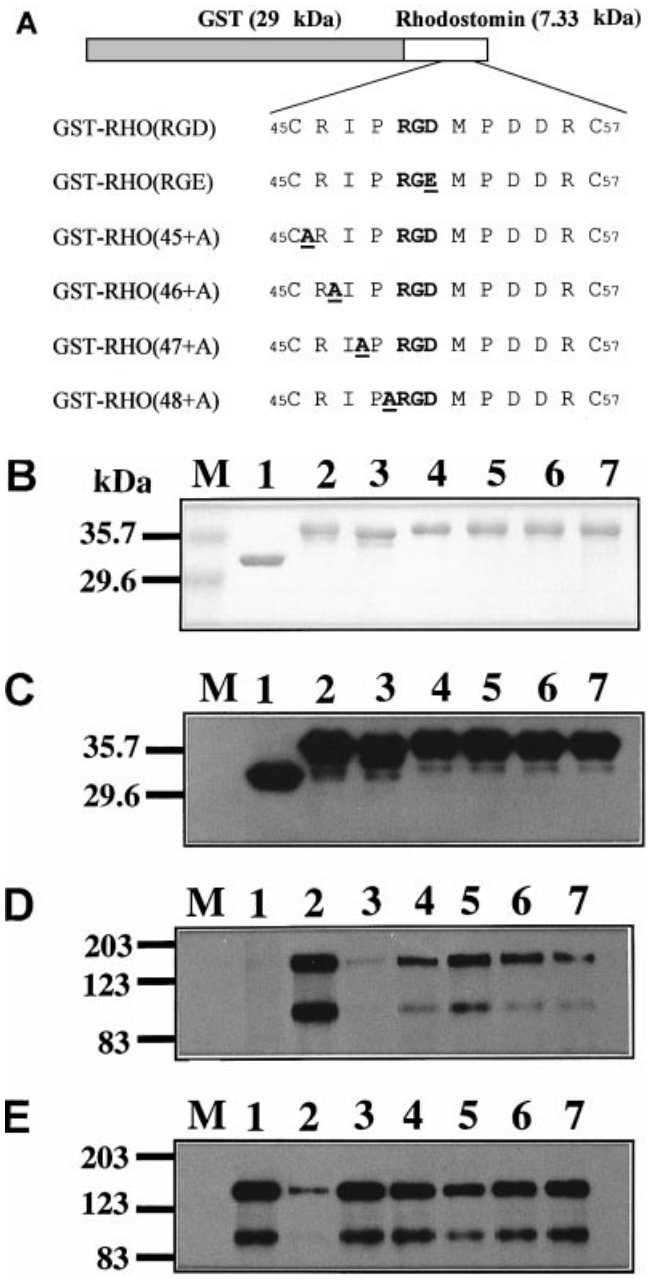

Figure 4 Non-reducing SDS/PAGE analysis of GST pull-down assays of insertion mutants of N-terminal region flanking the RGD motif

(**A**) A partial amino acid sequence of insertion mutants in the N-terminal region flanking RGD motif. Only the sequence of the RGD loop is shown. (**B**) The pull-down samples were analysed by non-reducing SDS/10.5% (w/v)-PAGE and stained with Coomassie Brilliant Blue. The theoretical size of GST is 29 kDa and the theoretical size of GST–RHO is 36.3 kDa. (**C**) The pull-down samples were analysed by non-reducing SDS/10.5%-PAGE and detected with anti-GST–RHO antiserum. (**D**) The pull-down samples were analysed by non-reducing SDS/9%-PAGE and detected by avidin–HRP ECL*. (**E**) The platelet lysate flowthrough of GST-, wild-type- or GST–RHO-mutant-coated beads was pulled down by GST–RHO(RGD); the second pull-down samples were analysed by non-reducing SDS/9%-PAGE and detected by avidin–HRP ECL. Lane 1, GST; lane 2, GST-RHO(RGD); lane 3, GST–RHO(RGE); lane 4, 45+A; lane 5, 46+A; lane 6, 47+A; lane 7, 48+A. Data are representative of three experiments.

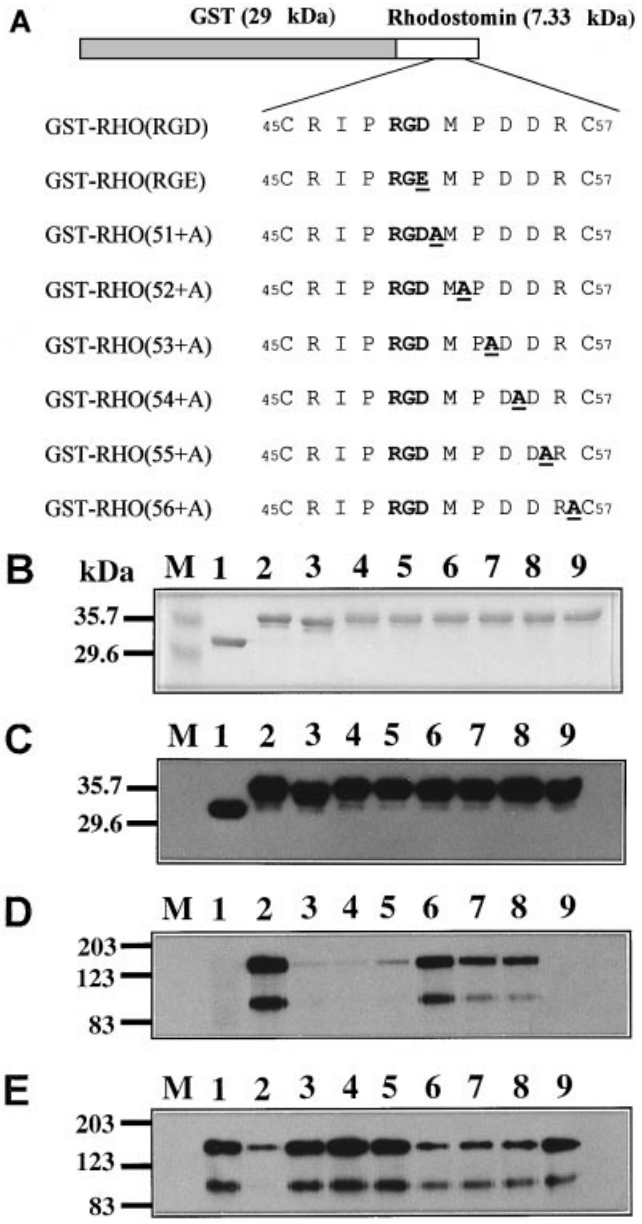

Figure 5 Non-reducing SDS/PAGE analysis of GST pull-down assays of insertion mutants of C-terminal region flanking the RGD motif

(**A**) A partial amino acid sequence of insertion mutants in the C-terminal region flanking RGD motif. Only the sequence of the RGD loop is shown. (**B**) The pull-down samples were analysed by non-reducing SDS/10.5% (w/v)-PAGE and stained with Coomassie Brilliant Blue. The theoretical size of GST is 29 kDa and the theoretical size of GST–RHO is 36.3 kDa. (**C**) The pull-down samples were analysed by non-reducing SDS/10.5%-PAGE and detected with anti-GST–RHO antiserum. (**D**) The pull-down samples were analysed by non-reducing SDS/9%-PAGE and detected by avidin–HRP ECL*. (**E**) The platelet lysate flowthrough of GST-, wild-type- or GST–RHO-mutant-coated beads were pulled down by GST–RHO(RGD); the second pull-down samples were analysed by non-reducing SDS/9%-PAGE and detected by avidin–HRP ECL*. Lane 1, GST; lane 2, GST–RHO(RGD); lane 3, GST–RHO(RGE); lane 4, 51+A; lane 5, 52+A; lane 6, 53+A; lane 7, 54+A; lane 8, 55+A; lane 9, 56+A. Data are representative of three experiments.

46+A, 47+A, 48+A, 53+A, 54+A and 55+A, did not exhibit such an effect, an obvious inhibition being only observed at a concentration of 1.0 μM, but not at 0.1 or 0.2 μM. Table 2 summarizes the inhibition effect of GST–RHO(RGD) and insertion mutants on thrombin-induced platelet aggregation. The inhibition ranged from 51 to 60% for mutants 54+A, 55+A, 53+A. 46+A, 47+A and 48+A, was close to 60% for wild-type and 35% for the 45+A. In contrast, 11–16% inhibition was observed for mutants 51+A and 52+A. The 56+A mutant showed no inhibition, neither did the mutant RGE and the negative control of GST. Thus the inhibition effect of each

Table 1 GST pull-down assays of GST–RHO insertion mutants

Biotinylated human platelet surface proteins were absorbed by GST–RHO(RGD) and related mutants. The pull-down samples were analysed by non-reducing SDS/9%-(w/v)-PAGE and detected by avidin–HRP ECL*. The bound integrins αIIb and β3 were estimated by densitometer. The integrin binding for each mutants was calculated from: binding = [first pull-down/(first pull-down + second pull-down)] × 100 (%). The relative activity was calculated from: activity = {(percentage integrin binding for each mutant)/[percentage integrin binding for GST–RHO(RGD)]}.

	Relative activity (%)		Loss of activity (%)	
GST-fusion protein	αIIb	β3	αIIb	β3
GST	9	1	91	99
GST–RHO(RGD)	100	100	0	0
GST–RHO(RGE)	3	0	97	100
GST–RHO(45+A)	33	16	67	84
GST–RHO(46+A)	57	54	43	46
GST–RHO(47+A)	34	16	66	84
GST–RHO(48+A)	30	8	70	92
GST	0	0	100	100
GST–RHO(RGD)	100	100	0	0
GST–RHO(RGE)	0	0	100	100
GST–RHO(51+A)	3	2	97	98
GST–RHO(52+A)	9	6	91	94
GST–RHO(53+A)	83	75	17	25
GST–RHO(54+A)	63	30	37	70
GST–RHO(55+A)	57	14	43	86
GST–RHO(56+A)	2	3	98	97

Table 2 Inhibition of thrombin-induced human platelet aggregation in the presence of GST–RHO insertion mutants

Platelet aggregation was measured as previously described. The percentage of inhibition was calculated using the absorbance for each test, the absorbance of diluent only after thrombin activation was used as 0% inhibition, while the absorbance for each test before thrombin activation was used as 100% inhibition. Results are means ± S.E.M. (n = 4).

		Inhibition of platelet aggregation (%)		
GST–RHO Insertion mutant	Concn. (μM) ...	0.1	0.2	1.0
GST		< 1	< 1	< 1
GST-RHO(RGD)		29 ± 1	46	60 ± 7
GST-RHO(RGE)		< 1	< 1	< 1
GST-RHO(45+A)		< 1	< 1	36 ± 8
GST-RHO(46+A)		< 1	6 ± 5	54 ± 5
GST-RHO(47+A)		< 1	2 ± 5	51 ± 6
GST-RHO(48+A)		< 1	5 ± 5	52 ± 7
GST-RHO(51+A)		< 1	< 1	11 ± 6
GST-RHO(52+A)		< 1	< 1	16 ± 4
GST-RHO(53+A)		< 1	4 ± 6	56 ± 6
GST-RHO(54+A)		< 1	4 ± 2	60 ± 2
GST-RHO(55+A)		< 1	4 ± 1	57 ± 10
GST-RHO(56+A)		< 1	< 1	< 1

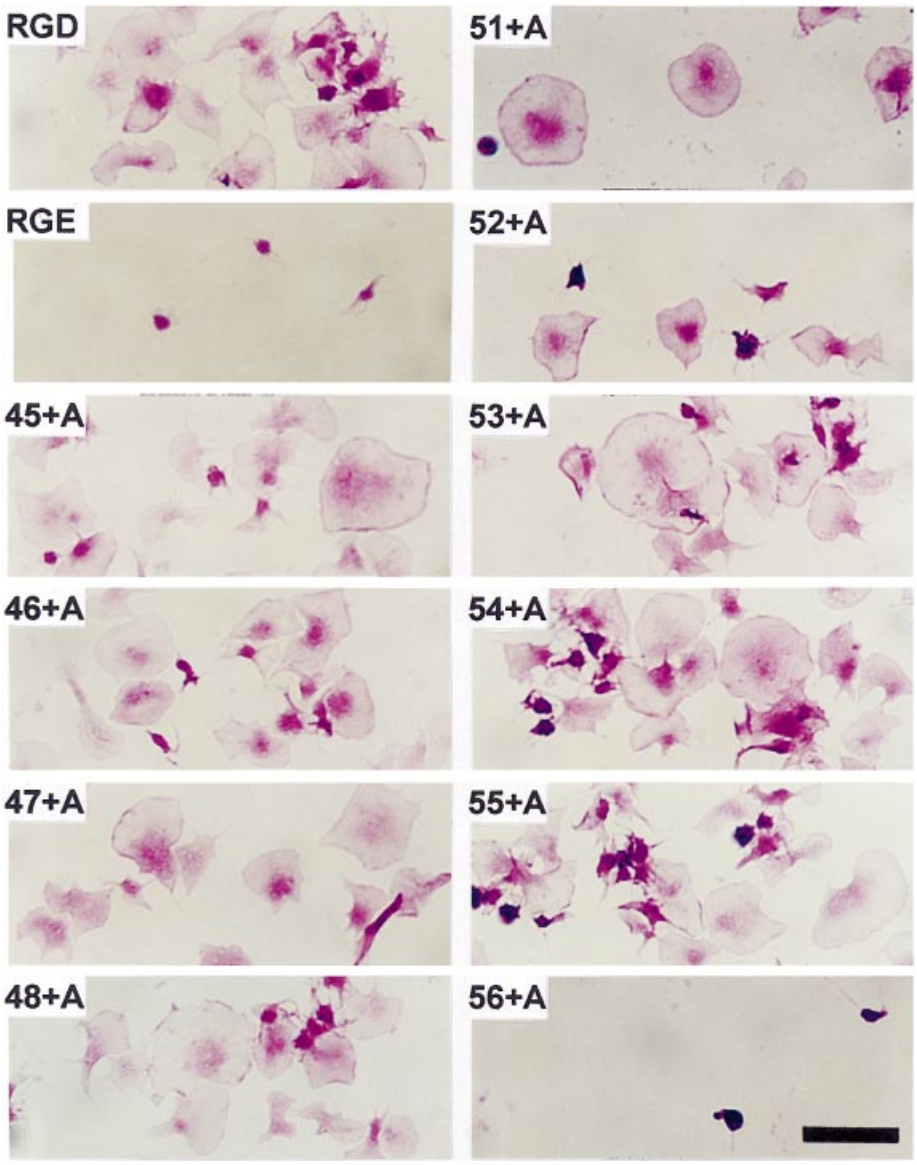

Figure 6 Platelet-attachment assays of insertion mutants

Platelets (1×10^6 cells/ml) were incubated on GST–RHO(RGD)- or insertion-mutant-coated coverslips at 37 °C for 15 min. After 15 min, the unattached cells were removed by gently washing; the attached cells were fixed and stained with Liu's stain. The GST-fusion protein which was coated on coverslips is indicated at the upper left of each picture. Representative micrographs are randomly obtained from three experiments and three different platelet donors. The bar represents 1 μm.

mutant was highly correlated with its ability to pull-down integrin αIIbβ3.

Number of platelets which attached and spread on 51 + A-, 52 + A- and 56 + A-coated coverslips is decreased

Platelet adhesion and spreading on RGD-containing substrates is another bioassay of GST–RHO. We previously have shown that GST–RHO(RGD) as adhesive substratum can induce platelets to fully spread, whereas GST and GST-RHO(RGE) cannot [31]. Therefore we examined the ability of each mutant to bind and spread platelets. As shown in Figure 6, the number of attached platelets on 51 + A-, 52 + A- and 56 + A-coated coverslips was much lower than on GST–RHO(RGD) and other insertion- mutant-coated coverslips. When the morphology of adhered platelets was examined, few platelets on 51 + A- and 52 + A-coated coverslips could be observed in the fully spread form. Notably, the platelets on 56 + A-coated coverslips did not spread at all and were similar to those on GST- and RGE-coated coverslips. The consistent results for each mutant obtained above indicate that the affinity of the RHO variants for integrin αIIbβ3 is tightly associated with the ability of the signal transduction in platelets to induce full spreading.

Although the structure of RHO has been determined by NMR spectroscopy, showing that the RGD sequence is located at the very tip of a loop [34] and the specific amino acids in RHO which influence the binding to integrin αIIbβ3 have been identified by alanine substitution [21], the importance of the length of RGD loop and the relative distance between flanking sequence and RGD on its binding to αIIbβ3 is largely unknown. In the present

study we have used the alanine-insertion approach to try to answer both these questions. If we compare this approach to the use of substitution mutagenesis of conservative or non-conservative amino acids, alanine-insertion mutagenesis may be able to reveal the effects of relative distance between specific residue and RGD motif on the functioning of the molecule. One possible problem might be that the insertion of alanine can affect the geometry of RGD loop. The results here indicate that there are only minor effects on N-terminal insertion of RGD motif and on 53+A, 54+A and 55+A (see Figures 4 and 5). The results show clearly that an increase in the RGD loop by one alanine residue does not dramatically affect RHO binding to αIIbβ3.

However, if the length of RGD-loop is increased or decreased by one residue such that the position of Pro^{53} is shifted, RHO functionality is greatly reduced. Since proline is often found in the bends of a folded protein, the alteration in the position of proline may induce conformational changes to the protein and this may affect its function. Nevertheless, this does not apply to proline at position 48, since the 47+A and 48+A mutants retain some degree of functionality. This observation is consistent with the alanine-substitution study in which substitution of Pro^{53} has a greater effect than substitution of Pro^{48} [21]. The hypothesis is also supported by the study of elegantin, a 72-amino-acid disintegrin. The flanking sequence of RGD in elegantin is ARGDNP [35,36] and has a conserved proline corresponding to Pro^{53}, but not to Pro^{48}. Another piece of supporting evidence for the importance of Pro^{53} in RHO comes from the NMR structure of dendroaspin, which is a 59-amino-acid neurotoxin with the same sequence of PRGDMP on loop III [37]. NMR spectroscopy reveals that the Pro^{47} of dendroaspin, which corresponds to the Pro^{53} of RHO, is a key residue that bends the backbone so that the RGD sequence is placed away from the bulk of the molecule [37]. Interestingly, the similarity of amino acid sequence between dendroaspin and RHO is less extensive than that between elegantin and RHO. Dendroaspin, but not elegantin, has the same action as RHO on platelet adhesion to fibrinogen [35].

In addition to the 51+A and 52+A mutants causing a dramatic decrease in binding to integrin, the 56+A mutant completely lost its ability to bind to integrin. This mutant seems to be more seriously affected, because it also completely loses its ability to inhibit platelet aggregation and to induce platelet spreading (see Table 2 and Figure 6). Because the 53+A, 54+A and 55+A mutants do not completely lose their ability to bind integrin, whereas the 56+A mutant does, it is unlikely that the loss of function of the 56+A mutant is due to the 'Cys^{57} position' effect. Since the six pairs of disulphide linkages in RHO have been suggested to play an important role in fixing the proper conformation of the molecule [34], it is suspected that the alanine insertion directly before Cys^{57} may influence the disulphide pairing. However, the 56+A mutant loses integrin-binding activity completely, whereas the 45+A mutant partially loses its functionality. The explanation of this difference in the influence on the disulphide pairing could be that Cys^{45} is linked to Cys^{64} at C-terminal tail, whereas the Cys^{57} is linked to the Cys^{32}; the former disulphide-bond formation is less restricted than the latter, which is more interior [34]. Thus a change in the more restricted disulphide bridge causes more structural change and thus loss of functionality. To test this hypothesis, a further study involving the generation of a 31+A and 56+A combination is needed to see if the binding activity of integrin will be restored or not.

We are grateful to Dr Y.-H. W. Lee [Institute of Biochemistry, National Yang-Ming University (NYMU)] and Dr R. Kirby (Visiting Professor in the Institute of Genetics, NYMU) for their critical review on the manuscript before its submission. Special thanks are due to Dr Chi-Hung Lin and Dr Woei-Jer Chuang for their helpful discussions. This work was supported by program project grants of RHO from the National Science Council (NSC88-2314-B010-057 and NSC89-2320-B010-019). An award by the National Science Council and the Medical Research and Advancement Foundation in Memory of Dr Chi-Shuen Tsou helped S.J.L. in this work.

REFERENCES

1 Tamkun, J. W., DeSimone, D. W., Fonda, D., Patel, R. S., Buck, C., Horwitz, A. F. and Hynes, R. O. (1986) Structure of integrin, a glycoprotein involved in the transmembrane linkage between fibronectin and actin. Cell **46**, 271–282
2 Hynes, R. O. (1987) Integrins: a family of cell surface receptors. Cell **48**, 549–554
3 Gumbiner, B. M. (1996) Cell adhesion: the molecular basis of tissue architecture and morphogenesis. Cell **84**, 345–357
4 Haas, T. A. and Plow, E. F. (1994) Integrin–ligand interactions: A year in review. Curr. Opin. Cell Biol. **6**, 656–662
5 Fassler, R., Georges-Labouesse, E. and Hirsch, E. (1996) Genetic analyses of integrin function in mice. Curr. Opin. Cell Biol. **8**, 641–646
6 Calvete, J. J. (1999) Platelet integrin GPIIb/IIIa: structure–function correlations. An update and lessons from other integrins. Proc. Soc. Exp. Biol. Med. **222**, 29–38
7 Parise, L. V. (1999) Integrin $\alpha_{IIb}\beta_3$ signaling in platelet adhesion and aggregation. Curr. Opin. Cell Biol. **11**, 597–601
8 Shattil, S. J., Ginsberg, M. H. and Brugge, J. S. (1994) Adhesive signaling in platelets. Curr. Opin. Cell Biol. **6**, 695–704
9 Ruoslahti, E. and Pierschbacher, M. D. (1986) Arg-Gly-Asp: a versatile cell recognition signal. Cell **44**, 517–518
10 Hynes, R. O. (1992) Integrins: versatility, modulation, and signaling in cell adhesion. Cell **69**, 11–25
11 Pierschbacher, M. D. and Ruoslahti, E. (1987) Influence of stereochemistry of the sequence Arg-Gly-Asp-Xaa on binding specificity in cell adhesion. J. Biol. Chem. **262**, 17294–17298
12 Hautanen, A., Gailit, J., Mann, D. M. and Ruoslahti, E. (1989) Effects of modifications of the RGD sequence and its context on recognition by the fibronectin receptor. J. Biol. Chem. **264**, 1437–1442
13 Rahman, S., Aitken, A., Flynn, G., Formstone, C. and Savidge, G. F. (1998) Modulation of RGD sequence motifs regulates disintegrin recognition of $\alpha_{IIb}\beta_3$ and $\alpha_5\beta_1$ integrin complexes. Biochem. J. **335**, 247–257
14 Gould, R. J., Polokoff, M. A., Friedman, P. A., Huang, T.-F., Holt, J. C., Cook, J. J. and Niewiarowski, S. (1990) Disintegrins: a family of integrin inhibitory proteins from viper venoms. Proc. Soc. Exp. Biol. Med. **195**, 168–171
15 Blobel, C. P. and White, J. M. (1992) Structure, function and evolutionary relationship of proteins containing a disintegrin domain. Curr. Opin. Cell Biol. **4**, 760–765
16 McLane, M. A., Marcinkiewicz, C., Vijay-Kumar, S., Wierzbicka-Patynowski, I. and Niewiarowski, S. (1998) Viper venom disintegrins and related molecules. Proc. Soc. Exp. Biol. Med. **219**, 109–119
17 Huang, T.-F. (1998) What have snakes taught us about integrins? Cell. Mol. Life Sci. **54**, 527–540
18 Huang, T.-F., Wu, Y.-J. and Ouyang, C. (1987) Characterization of a potent platelet aggregation inhibitor from *Agkistrodon rhodostoma* snake venom. Biochim. Biophys. Acta **925**, 248–257
19 Dennis, M. S., Henzel, W. J., Pitti, R. M., Lipari, M. T., Napier, M. A., Deisher, T. A., Bunting, S. and Lazarus, R. A. (1990) Platelet glycoprotein IIb-IIIa protein antagonists from snake venoms: Evidence for a family of platelet-aggregation inhibitors. Proc. Natl. Acad. Sci. U.S.A. **87**, 2471–2475
20 Liu, C.-Z., Wang, Y.-W., Shen, M.-C. and Huang, T.-F. (1994) Analysis of human platelet glycoprotein IIb-IIIa by fluorescein isothiocyanate-conjugated disintegrins with flow cytometry. Thromb. Haemostasis **72**, 919–925
21 Dennis, M. S., Carter, P. and Lazarus, R. A. (1993) Binding interactions of kistrin with platelet glycoprotein IIb-IIIa: Analysis by site-directed mutagenesis. Proteins Struct. Funct. Genet. **15**, 312–321
22 Scarborough, R. M., Rose, J. W., Naughton, M. A., Phillips, D. R., Nannizzi, L., Arfsten, A., Campbell, A. M. and Charo, I. F. (1993) Characterization of the integrin specificities of disintegrins isolated from American pit viper venoms. J. Biol. Chem. **268**, 1058–1065
23 Scarborough, R. M., Naughton, M. A., Teng, W., Rose, J. W., Phillips, D. R., Nannizzi, L., Arfsten, A., Campbell, A. M. and Charo, I. F. (1993) Design of potent and specific integrin antagonists. Peptide antgonists with high specificity for glycoprotein IIb-IIIa. J. Biol. Chem. **268**, 1066–1073
24 Lu, X., Rahman, S., Kakkar, V. V. and Authi, K. S. (1996) Substitutions of proline 42 to alanine and methionine 46 to asparagine around the RGD domain of the neurotoxin dendroaspin alter its preferential antagonism to that resembling the disintegrin elegantin. J. Biol. Chem. **271**, 289–294

25 Scaloni, A., Di Martino, E., Miraglia, N., Pelagalli, A., Della Morte, R., Staiano, N. and Pucci, P. (1996) Amino acid sequence and molecular modelling of glycoprotein IIb-IIIa and fibronectin receptor isoantagonists from *Trimeresurus elegans* venom. Biochem. J. **319**, 775–782
26 Chang, H.-H., Tsai, W.-J. and Lo, S. J. (1997) Glutathione *S*-transferase–RHO fusion protein inhibits platelet aggregation and induces platelet shape change. Toxicon **35**, 195–204
27 Chang, H.-H., Chang, C.-P., Chang, J.-C., Dung, S.-Z. and Lo, S. J. (1997) Application of recombinant RHO in studying cell adhesion. J. Biomed. Sci. **4**, 235–243
28 Chang, H.-H., Hu, S.-T., Huang, T.-F., Chen, S.-H., Lee, Y.-H. W. and Lo, S. J. (1993) RHO, an RGD-containing peptide expressed from a synthetic gene in *Escherichia coli*, facilitates the attachment of human hepatoma cells. Biochem. Biophys. Res. Commun. **190**, 242–249
29 Mustard, J. F., Kinlough-Rathbone, R. L. and Packham, M. A. (1989) Isolation of human platelet from plasma by centrifugation and washing. Methods Enzymol. **169**, 3–11
30 Towbin, H., Staehelin, T. and Gordon, J. (1979) Electrophoretic transfer of proteins from polyacrylamide gels to nitrocellulose sheets: procedure and some applications. Proc. Natl. Acad. Sci. U.S.A. **76**, 4350–4354
31 Chang, H.-H., Lin, C.-H. and Lo, S. J. (1999) Recombinant RHO substrates induce human platelet full transformation and active calcium oscillation. Exp. Cell Res. **250**, 387–400
32 Chang, T.-C., Kou, S.-H., Chen, F.-W., Chang, C.-C., Liaw, K.-Y., Chang-Chien, Y., Huang, T.-S., Lin, C.-C. and How, S.-W. (1982) Cytopathology of thyroid cancer by fine needle aspiration with Liu's stain. J. Formosan Med. Assoc. **81**, 1404–1412
33 Du, X., Plow, E. F., Frelinger, III, A. L., O'Toole, T. E., Loftus, J. C. and Ginsberg, M. H. (1991) Ligands "activate" integrin $\alpha_{IIb}\beta_3$ (platelet GPIIb-IIIa). Cell **65**, 409–416
34 Adler, M., Lazarus, R. A., Dennis, M. S. and Wagner, G. (1991) Solution structure of kistrin, a potent platelet aggregation inhibitor and GP IIb-IIIa antagonist. Science **253**, 445–448
35 Rahman, S., Lu, X., Kakkar, V. V. and Authi, K. S. (1995) The integrin $\alpha_{IIb}\beta_3$ contains distinct and interacting binding sites for snake-venom RGD (Arg-Gly-Asp) proteins. Biochem. J. **312**, 223–232
36 Rahman, S., Flynn, G., Aitken, A., Patel, Y., Hussain, F., Lu, X., Loftus, J. C., French, D., Wijelath, E., Strand, K. and Savidge, G. F. (2000) Differential recognition of snake venom proteins expressing specific Arg-Gly-Asp (RGD) sequence motifs by wild-type and variant integrin $\alpha_{IIb}\beta_3$: further evidence for distinct sites of RGD ligand recognition exhibiting negative allostery. Biochem. J. **345**, 701–709
37 Sutcliffe, M. J., Jaseja, M., Hyde, E. I., Lu, X. and Williams, J. A. (1994) Three-dimensional structure of the RGD-containing neurotoxin homologue dendroaspin. Nat. Struct. Biol. **1**, 802–807

Received 13 November 2000/2 March 2001; accepted 19 April 2001